PUBLICATIONS OF THE ASTRONOMICAL SOCIETY OF THE PACIFIC, **122**:1311–1319, 2010 November

Algol-Type Eclipsing Binaries with δ Scuti-Type Pulsating Components: IV Cas

SEUNG-LEE KIM, JAE WOO LEE, CHUNG-UK LEE, AND JAE-HYUK YOUN

Korea Astronomy and Space Science Institute, Daejeon 305-348, Korea; slkim@kasi.re.kr, jwlee@kasi.re.kr, leecu@kasi.re.kr, jhyoon@kasi.re.kr

Received 2010 May 6; accepted 2010 September 9; published 2010 October 7

ABSTRACT. We present the results of photometric and spectroscopic observations of the Algol-type eclipsing binary with a δ Scuti-type pulsating component IV Cas. This is the first comprehensive study of the absolute properties of the binary system and also of the pulsation characteristics of the primary component. The high-resolution spectroscopic data have enabled us to estimate the atmospheric parameters of the primary component. Our BV light-curve analysis has revealed that the binary system is in a semidetached configuration, consisting of a detached main-sequence primary of spectral type A3 and an evolved secondary of early-K spectral type, which fills its inner Roche lobe completely. We found that the two components are too close to each other to form an accretion disk. Spectroscopic results without an emission feature supported the nonexistence of noticeable disk. The rotation of the primary turned out to be nearly synchronized with the revolution, giving a hint that IV Cas is in the middle or late stage of the slow mass transfer phase. This coincides well with a slow mass transfer rate deduced from the fact that there was no secular parabolic change of the orbital period for the past ~100 yr. Using residuals subtracted from synthetic eclipsing curves of photometric data, we examined the pulsation properties of the primary component. A multiple-frequency analysis was applied to the residuals in the out-of-primary eclipsing phases and this resulted in the detection of four frequencies: $f_1 = 32.69236$ cycles day^{-1}, $f_2 = 36.65999$ cycles day^{-1}, $f_3 = 20.71649$ cycles day^{-1}, and $f_4 = 30.66072$ cycles day^{-1}. We tentatively identified their pulsation modes on the basis of pulsation constants, frequency spacing, mode visibility in eclipsing binaries, phase differences, and amplitude ratios; f_1 and f_4 (or f_1 and f_2) appeared to be rotational splitting frequencies. The observational properties of IV Cas well matched the empirical relations for Algol-type eclipsing binaries with δ Scuti-type pulsating components.

Online material: color figures

1. INTRODUCTION

Physical processes in the stellar interior play a key role in stellar evolution. Asteroseismology is used to investigate the internal parts of stars by means of their pulsation features and can therefore give us very important physical constraints on stellar evolution (see review articles on asteroseismology by Brown & Gilliland 1994; Cunha et al. 2007). The success of helioseismological approaches to the Sun based on the huge number of oscillating modes of about 10^7 encourages asteroseismologists to make similar attempts on stars, comparing the observed pulsation frequencies with theoretical ones. But the limited number of observable frequencies for stars makes it much harder to obtain successful results. This is the reason why further stellar properties are required to reduce the number of free parameters in theoretical models. In this sense, pulsators in stellar systems (i.e., components of binary/multiple systems or members of star clusters) are very attractive targets for asteroseismology because their physical properties such as masses, radii, and ages can be determined accurately from system parameters and independently of pulsation model (Lampens 2006; Pigulski 2006).

The δ Scuti-type pulsating stars have been regarded as one of a few major types of variables for asteroseismic studies due to their multiple periodicity (Brown & Gilliland 1994; Breger 2000). Mkrtichian et al. (2004) introduced a new variable group, the (B)A-F spectral type mass-accreting main-sequence pulsating stars in semidetached Algol-type eclipsing binary systems, as an oscillating Algol-type eclipsing binary (oEA). The oEA stars have nearly the same pulsating characteristics as δ Scuti stars but have experienced a very different evolution process, which originates from mass transfer in a semidetached binary system. They are important from an asteroseismological point of view, because we can estimate their physical parameters directly from the eclipsing binary properties.

Rodríguez et al. (2000) presented an extensive catalog of δ Scuti and related stars. Among 636 stars listed in the catalog, only nine stars are components in eclipsing binary systems. Later, Soydugan et al. (2006b) listed 25 eclipsing binaries with δ Scuti-type components; nearly one-third of them were discovered in our photometric survey from 2002 to 2005 (Kim et al. 2003, 2005). Thereafter, several discoveries have been reported and the number of them has increased up to ~35 stars; recent examples include GSC 4588-0883 by Dimitrov et al. (2009),

TY Cap and WY Cet by Liakos & Niarchos (2009), and DY Aqr and BG Peg by Soydugan et al. (2009). Only five of the ~35 stars have been investigated photometrically or spectroscopically in detail: CT Her by Lampens et al. (2010), Y Cam by Kim et al. (2002) and by Rodríguez et al. (2010), RZ Cas by Rodríguez et al. (2004a) and by Lehmann & Mkrtichian (2008), AB Cas by Rodríguez et al. (2004b), and AS Eri by Mkrtichian et al. (2004).

IV Cas (=2MASS J23493152 + 5308046, $V = 11.245$ mag, $B - V = 0.387$ mag) has been known as a semidetached Algol-type eclipsing binary in the GCVS catalog (Samus et al. 2009). The oEA-type pulsating features of IV Cas were discovered in our photometric survey (Kim et al. 2005). Wolf et al. (2006) examined the orbital period change of IV Cas and found a sinusoidal variation in the O-C diagram. They interpreted the variation as a light-travel time effect by the third component with minimum mass of $0.96\ M_{\odot}$. Although a few tens of eclipsing minimum epochs were reported by many observers, a detailed light-curve analysis of IV Cas has not been presented yet. The probable reason is that its orbital period is close to 1.0 day, requiring a very long observation time at a single site in order to cover full orbital phases. In this article, we present the first eclipsing light-curve analysis of IV Cas and the pulsation characteristics of the primary component in detail, based on dual-site photometric observations and high-resolution spectroscopic data.

2. OBSERVATIONS AND DATA REDUCTION

We performed photometric observations during 17 nights between 2004 November and 2006 September at two sites in the Sobaeksan Optical Astronomy Observatory (SOAO) in Korea and in the Mount Lemmon Optical Astronomy Observatory (LOAO) in Arizona. The Korea Astronomy and Space Science Institute has been operating the SOAO 61 cm and LOAO 1.0 m telescopes used in this study. The two sites with an 8 hr difference in time zones enable us to observe a target uninterruptedly for about 17 hr a day. This gives the great advantage of a more complete coverage of orbital phases for eclipsing binaries like IV Cas with orbital periods close to 1.0 day. The specification of the instrument and reduction process of CCD images have been described by Kim et al. (2003, 2005). Typical seeing size of the stellar images was about 3.5" for the SOAO data and about 2.3" for the LOAO during the observing run. Aperture radius for photometry was adopted as about twice the seeing. Table 1 shows the observation log.

Differential magnitudes were calculated by the standard differential photometric method using a comparison star and several reference stars in the same field of observation. GSC 4001-1876 (=2MASS J23500471 + 5315495, $V = 11.428$ mag, and $B - V = 0.631$ mag) with brightness and color index similar to the variable IV Cas (V) was chosen as the comparison star (C). The data obtained simultaneously at the two sites were overlapped during three nights near HJD 2,453,686.9, 2,453,689.9, and 2,453,690.9. No systematic magnitude difference between the two sites was detected. Table 2 shows short samples of differential magnitudes: namely, $m(V) - m(C)$. Full data are available in the online version of this article or upon request from the first author. The 1-σ value of the dispersion for differential magnitudes between the comparison star and one of the reference stars, GSC 4001-0188 (=2MASS J23490774 + 5316040, $V = 11.125$ mag, and $B - V = 0.986$ mag), was estimated to be 0.005 mag.

TABLE 1
PHOTOMETRIC OBSERVATION LOG OF IV CAS

Date (UT)	HJD (2,453,000.0+)	N (B)	N (V)	Observatory
2004 11 27	336.79 ~ 336.87	73	0	LOAO
2004 11 29	338.72 ~ 338.80	45	0	LOAO
2004 11 30	339.69 ~ 339.83	91	0	LOAO
2004 12 15	354.55 ~ 354.65	90	0	LOAO
2005 11 12	686.55 ~ 686.92	54	52	LOAO
2005 11 13	687.56 ~ 687.92	170	170	LOAO
2005 11 14	688.55 ~ 688.69	65	64	LOAO
2005 11 15	689.57 ~ 689.93	165	165	LOAO
2005 11 16	690.56 ~ 690.92	279	0	LOAO
2005 10 17	660.94 ~ 660.98	11	0	SOAO
2005 11 12	686.90 ~ 687.28	140	139	SOAO
2005 11 14	688.91 ~ 689.27	122	121	SOAO
2005 11 15	689.92 ~ 690.27	118	118	SOAO
2005 11 16	690.91 ~ 691.26	224	29	SOAO
2005 11 17	691.89 ~ 692.26	318	0	SOAO
2006 9 2	980.96 ~ 981.22	101	102	SOAO
2006 9 3	981.96 ~ 982.20	89	92	SOAO
17 nights	104 hr	2155	1052	...

A total of 2155 individual data points in the B band and 1052 points in the V band were collected and gathered, mainly during the 2005 observation season; 299 B-band data obtained with the LOAO in 2004 had already been used in the discovery report by Kim et al. (2005). Figure 1 shows a phase diagram of IV Cas in the B and V bands. Orbital phases were calculated from our new light elements for the primary minimum, Pri.Min. =

TABLE 2
SHORT SAMPLES OF DIFFERENTIAL MAGNITUDES OF IV CAS

HJD[a]	ΔB	HJD[a]	ΔV
336.78994	−0.686	686.55344	+0.350
336.79132	−0.692	686.55580	+0.398
336.79268	−0.696	686.55816	+0.448
336.79405	−0.700	686.56053	+0.498
336.79541	−0.703	686.56289	+0.543
336.79679	−0.703	686.56525	+0.595
336.79816	−0.703	686.56761	+0.643
336.79984	−0.709	686.56997	+0.694
336.80097	−0.702	686.82315	−0.467
336.80210	−0.705	686.82551	−0.460

[a] HJD $2,453,000.0+$.

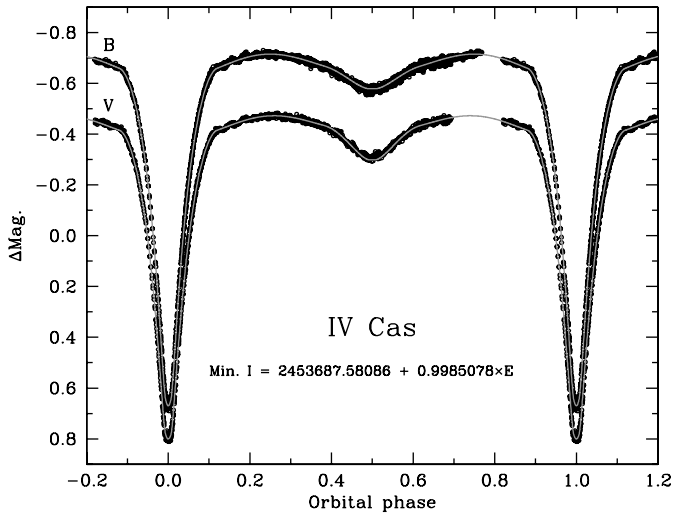

FIG. 1.—BV phase diagram of IV Cas. Dots represent observed data and solid lines representt synthetic curves from the WD code (Wilson & Devinney 1971). In spite of the orbital period being very close to 1.0 day, we could obtain nearly full light curves from dual-site observations with an 8 hr difference in time zones. See the electronic edition of the *PASP* for a color version of this figure.

HJD $2,453,687.58086(3) + 0.9985078(2) \times E$. The values in parentheses are standard deviations of the elements. Most of the orbital phases had good coverage to analyze the eclipsing light curve, although our observations missed around the secondary maximum of the phase ~ 0.8.

We obtained a high-resolution spectrum of IV Cas to estimate its atmospheric parameters such as effective temperature and surface gravity. To our knowledge, this is the first spectrum of IV Cas and no other spectroscopic study has been carried out before. The observation was made on 2005 November 30, using the echelle spectrograph BOES (Kim et al. 2006a) attached to the 1.8 m telescope at Bohyunsan Optical Astronomy Observatory in Korea. We used the same instrument setting and data reduction process as used by Lee et al. (2008). The largest fiber of 300 μm was chosen to give a resolving power of 30,000. Exposure time was 3600 s and the middle of the exposure was HJD 2,453,705.12694, corresponding to an orbital phase of 0.57.

3. BINARY PROPERTIES

3.1. Spectroscopic Results

Figure 2 displays the high-resolution spectrum of IV Cas over four spectral ranges of special interest. The line-strength ratios of Ca I λ4226 versus Fe II λ4233 and of Mg I triplets λ5167-72-83 are good temperature indicators for spectral type A stars. The ratios of IV Cas were similar to those of the A2V star HD 97633; spectra of several radial velocity standard stars like HD 97633 were obtained during the same night of observation. Mg II λ4481 and H_α λ6563 lines were utilized for deriving the rotational velocity and for examining emission features, respectively.

The stellar spectral synthesis program SPECTRUM by Gray & Corbally (1994) and the stellar atmosphere model by Kurucz (1993) were used to estimate the atmospheric parameters of IV Cas. We found the best-fitting parameters for the observed spectrum by an iterative method: effective temperature $T_{\rm eff} = 8500 \pm 250$ K, surface gravity $\log g = 4.0 \pm 0.5$, and projected rotational velocity $v_{\rm rot} \sin i_{\rm rot} = 115 \pm 5$ km s^{-1}, assuming solar metal abundance. The errors came from the model grid intervals we used. The surface gravity value was less sensitive to the spectrum than the other parameters, and so it was deduced from the results of the light-curve synthesis (see Table 3). These parameters correspond to those of a spectral type A3V star. For verification of the preceding method, we also estimated atmospheric parameters of HD 97633 to be $T_{\rm eff} = 9500 \pm 250$ K, $\log g = 3.5 \pm 0.5$, and $v_{\rm rot} \sin i_{\rm rot} = 23 \pm 1$ km s^{-1}, which coincided well with those in the literature (for example, Le Borgne et al. 2003; Royer et al. 2007).

The preceding atmospheric parameters of IV Cas should come from the hot primary component, because we obtained the spectrum at an orbital phase of 0.57 near the secondary minimum, during which the cool secondary is eclipsed by the hot primary component. Furthermore, the light contribution from the secondary component is only about 4% in the B band (see Table 3). We could not find any spectral line like the CH band λ4300, which originates from the cool secondary, most probably due to its very low brightness. Figure 2 shows that the observed H_α λ6563 line is well fitted with the synthetic absorption one. Contrary to the other oEA star AB Per, which showed a strong emission at H_α λ6563 (Kim et al. 2006b), we could not detect any emission feature of IV Cas at spectral lines between 3500 Å and 9000 Å. This implies that there is no noticeable accretion disk around the primary component of IV Cas.

3.2. Light-Curve Synthesis

The shape of the light curves in Figure 1 is superficially similar to that of β Lyr-type eclipsing binaries. A large difference between the primary and secondary eclipse depths indicates a significant temperature difference between the two components. In order to obtain reasonable parameters for the binary system, we simultaneously analyzed our BV light curves with the Wilson-Devinney binary code (Wilson & Devinney 1971, hereafter WD). For this synthesis, an effective temperature of $T_{\rm eff,1} = 8500$ K for the primary component was assumed from the former spectroscopic result. The logarithmic bolometric (X, Y) and monochromatic (x, y) limb-darkening coefficients were interpolated from the values of Van Hamme (1993) in concert with the atmosphere model option. Throughout the analysis, the light curves were modeled similarly to those of the eclipsing binaries XX Cep (Lee et al. 2007) and GW Gem (Lee et al. 2009). The adjustable parameters were the orbital

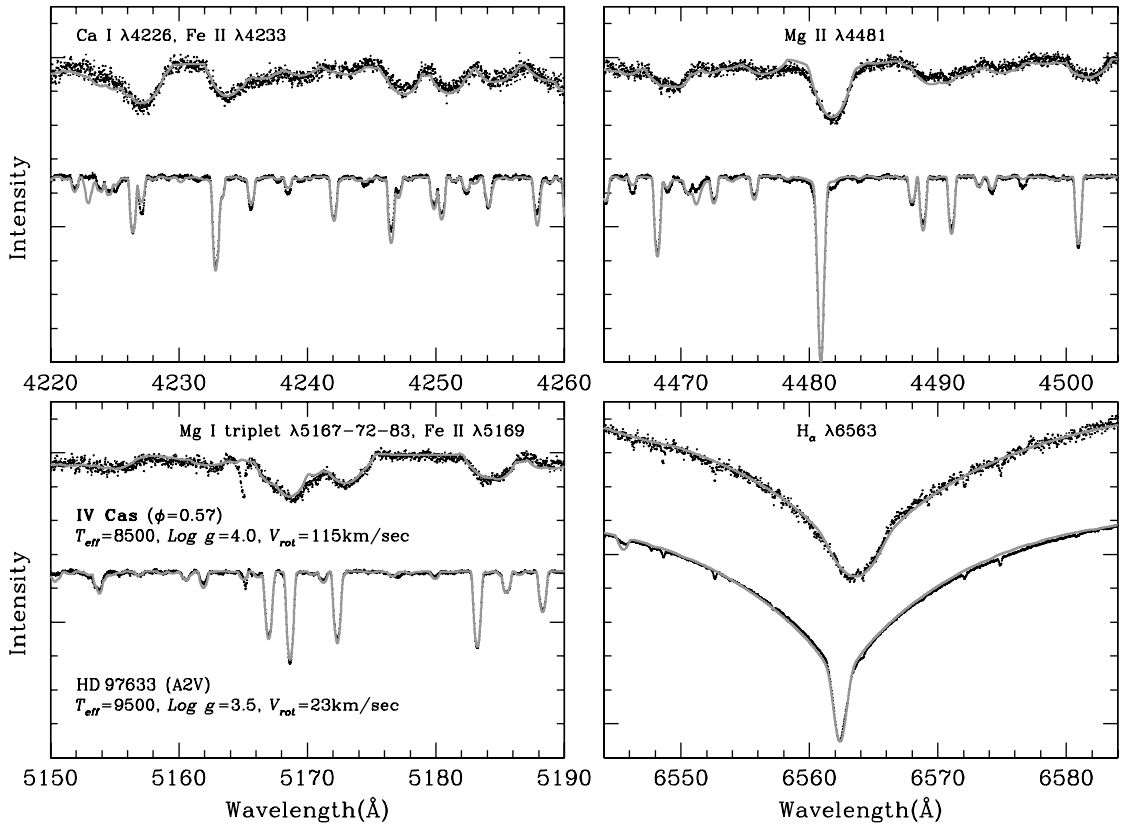

FIG. 2.—High-resolution spectrum of IV Cas over four spectral ranges of special interest. The spectrum was obtained at the orbital phase of 0.57. Dots represent observed data and solid lines synthetic curves from the SPECTRUM code (Gray & Corbally 1994). Spectra of HD 97633 are also displayed for comparison. See the electronic edition of the *PASP* for a color version of this figure.

ephemeris (T_0 and $P_{\rm orb}$), orbital inclination (i), temperature of the secondary star ($T_{\rm eff,2}$), dimensionless surface potentials (Ω), and monochromatic luminosity (L).

No reliable binary parameters for IV Cas have been known up to now. First, a photometric q-search procedure was conducted over the range of $0.15 \leq q \leq 0.70$ and the method of multiple subsets (Wilson & Biermann 1976) was employed to ensure the stability of our solution. For each assumed mass ratio, the WD calculation started from mode 2 (detached system) but always converged on mode 5 (semidetached system with secondary component filling its inner Roche lobe). The weighted sum of squared residuals reached a minimum at around $q = 0.40$. Then this value was treated as an adjustable parameter in subsequent calculations to derive a photometric solution. The results are plotted as solid lines in Figure 1 and listed in Table 3, wherein the values of the darkening coefficients for the secondary star have been changed to agree with the temperature of that component. The errors in the table were yielded from the WD code and may probably be underestimated. Finally, we looked for a possible third light source, as suggested by the previous orbital period study (Wolf et al. 2006), but found that the parameter remains indistinguishable

TABLE 3
BINARY PARAMETERS OF IV CAS CALCULATED FROM THE WD CODE

Parameters	Primary	Secondary
T_0 (HJD)	2,453,687.58086 ± 0.00003	...
$P_{\rm orb}$ (d)	0.9985078 ± 0.0000002	...
q	0.4077 ± 0.0009	...
i (deg)	87.47 ± 0.05	...
$T_{\rm eff}$ (K)	8500	5193 ± 7
Ω	3.252 ± 0.001	2.694
A	1.0	0.5
g	1.0	0.32
X, Y	0.659, 0.144	0.644, 0.177
x_B, y_B	0.784, 0.307	0.851,0.026
x_V, y_V	0.677, 0.281	0.792, 0.156
$L/(L_1+L_2)_B$	0.9600 ± 0.0004	0.0400
$L/(L_1+L_2)_V$	0.9225 ± 0.0006	0.0775
r (pole)	0.3487 ± 0.0002	0.2840 ± 0.0002
r (point)	0.3771 ± 0.0003	0.4089 ± 0.0008
r (side)	0.3600 ± 0.0002	0.2961 ± 0.0002
r (back)	0.3693 ± 0.0002	0.3287 ± 0.0002
r (volume)[a]	0.3596	0.3042

[a] Mean-volume radius.

from zero within the error. Residuals of the WD binary solution were 0.0087 mag in the B band and 0.0083 mag in V, which is a little larger than the estimated observational error of 0.005 mag (see § 2). This difference may be due to another variability source, i.e., pulsation of the primary component described in § 4.

The light-curve solutions indicate that IV Cas is in a semi-detached configuration, with the primary star filling about 83% of its inner Roche lobe and the secondary completely filling its limiting lobe. Although there is no spectroscopic orbital element, the absolute dimensions of the system can be roughly computed from our photometric results and from Harmanec's (1988) relation for mass as a function of spectral type. By assuming the primary star to be a normal main-sequence star of spectral type A3V and by adopting $T_{\odot} = 5780$ K for the solar value, we estimated the absolute parameters for both components given in Table 4. Here, the radii and luminosities were calculated by using the mean-volume radii for each component. The absolute parameters do not differ greatly from the approximate values estimated by Svechnikov & Kuznetsova (1990, cf. $M_1 = 2.15\ M_{\odot}$, $M_2 = 1.10\ M_{\odot}$, $R_1 = 2.00\ R_{\odot}$, and $R_2 = 1.95\ R_{\odot}$).

3.3. Orbital Period Variation

We examined the orbital period variation of IV Cas by means of the O-C diagram. Eleven new minimum epochs in Table 5 have been obtained from our data by Kwee & van Woerden's (1956) method. Our timings and four recent studies (Brát et al. 2008; Hübscher et al. 2009; Erkan et al. 2010) were very well matched with the previous O-C variation tendency to show only a sinusoidal curve (Wolf et al. 2006). We constructed the O-C diagram using a total of 297 epochs, combining our measurements with those in the literature, and consequently obtained nearly the same results as Wolf et al. (2006), so these are not described in detail. No secular parabolic change of the orbital period was detected for the past ~100 yr.

4. PULSATION PROPERTIES

4.1. Frequency Analysis

Our BV photometric data were utilized to investigate the pulsation properties of IV Cas. At first, we calculated residuals by subtracting the synthetic eclipsing curves (*solid lines in Fig. 1*) from the data. Next, the low-order polynomial fitting method was applied in order to reduce the low-frequency term caused by the imperfect synthetic curve fitting and/or by nightly variation of observation conditions. The residuals showed sinusoidal curves with an amplitude varying from cycle to cycle, indicating that multiple periods are superimposed.

TABLE 4

ABSOLUTE PARAMETERS OF IV CAS

Parameters	Primary	Secondary
$M\ (M_{\odot})$	1.98 ± 0.10	0.81 ± 0.04
$R\ (R_{\odot})$	2.13 ± 0.04	1.80 ± 0.03
$\log g$	4.08 ± 0.03	3.83 ± 0.03
$\log L/L_{\odot}$	1.33 ± 0.05	0.32 ± 0.05
$M_{\rm bol}$ (mag)	1.43 ± 0.13	3.94 ± 0.13

TABLE 5

NEW TIMES OF MINIMUM LIGHT FOR IV CAS

HJD	Error	Filter	Minimum type
2,453,354.58432	±0.00035	B	II
2,453,687.07985	±0.00058	B, V	II
2,453,687.58116	±0.00004	B, V	I
2,453,688.57959	±0.00005	B, V	I
2,453,689.07906	±0.00074	B, V	II
2,453,690.07460	±0.00080	B, V	II
2,453,690.57654	±0.00013	B, V	I
2,453,691.07319	±0.00043	B	II
2,453,692.07785	±0.00037	B	II
2,453,981.14219	±0.00006	B, V	I
2,453,982.14081	±0.00005	B, V	I

In a multiple-frequency analysis, we applied the discrete Fourier transform (DFT) and a least-squares fitting of the light curve (upgrade version of the program in Kim & Lee 1996). Our analysis yielded identical results to the computation package PERIOD04 by Lenz & Breger (2005). Since the primary component of IV Cas is a spectral type A3V star and was discovered to be a δ Scuti-type pulsator (Kim et al. 2005), we excluded the data around the primary minimum phases from 0.9 to 1.1, during which the primary component is eclipsed by the secondary and the pulsating light curves should be distorted.

The pulsation amplitude of the primary component can be diluted by the light contribution from the secondary. The dilution effect varies with orbital phases, with the largest at out-of-eclipse phases and the smallest at the secondary minimum. Although this can result in false periodicities in the DFT power spectra (Mkrtichian et al. 2004), we did not correct for the effect, which is assumed to be negligible, because the secondary accounts for only 4% of total luminosity of the binary system in the B band (see Table 3). When we tested the effect by using artificial data to increase the pulsation amplitudes around the secondary minimum phase, the powers of false $1/P_{\rm orb}$ splitting frequencies increased as expected, but the increment were small enough to be negligible in our real data.

Power spectra calculated from the DFT are shown in Figure 3. The spectral window is in the first panel. The 1.0 cycle day^{-1} side lobes appeared well, as is usual for data observed from a single observatory (Breger 2000). But our dual-site observations made the powers of the side lobes decrease down to about 35% of the main peak. The powers also included another aliasing effect caused by the primary eclipse gaps of $P_{\rm orb} \sim 1.0$ day interval for IV Cas, since we excluded data around the primary minimum phase.

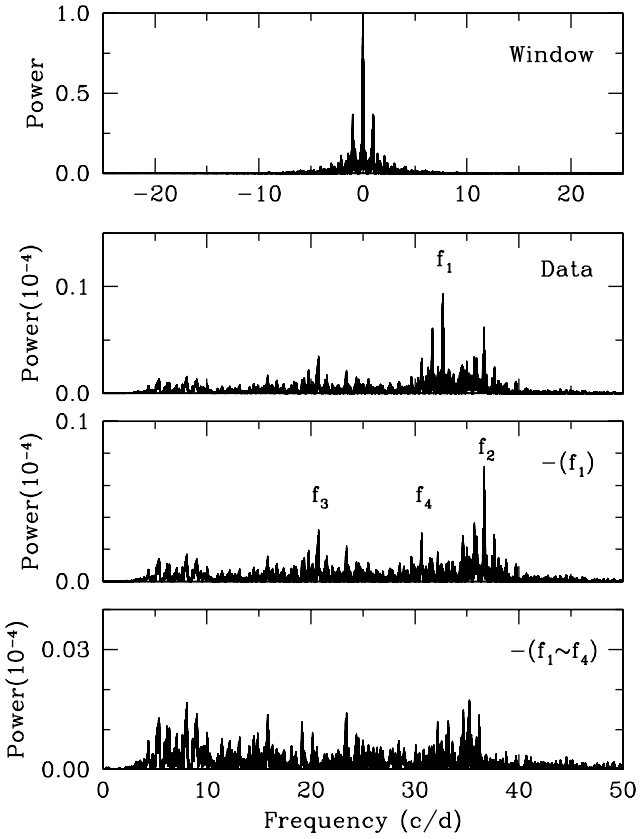

FIG. 3.—Power spectra of B-band residuals in the out-of-primary eclipsing phases. The window spectrum is displayed in the top panel. We could detect four frequencies in the next three panels.

After successive prewhitening of each frequency peak in the next three panels, we detected four frequencies at $f_1 = 32.69236 \pm 0.00008$ cycles day^{-1} (i.e., a dominant period of 44.05 minutes), $f_2 = 36.65999 \pm 0.00007$ cycles day^{-1}, $f_3 = 20.71649 \pm 0.00010$ cycles day^{-1}, and $f_4 = 30.66072 \pm 0.00013$ cycles day^{-1}. Some additional peaks near 35.2, 8.1 and 23.4 cycles day^{-1} still exist in the last panel. But we did not consider them to be significant, because they have smaller signal-to-noise amplitude ratios than the empirical criterion of 4.0 proposed by Breger et al. (1993) and could not be detected in the V-band data. Detailed results of the analysis are summarized in Table 6. Figure 4 displays light variations of the residuals in the B band and synthetic curves computed from the analysis.

4.2. Pulsation Mode

We attempted to identify the pulsation modes of four frequencies. The radial order n can be deduced by comparing theoretical and observed pulsation constants. Using the absolute parameters of $\log g$ and $M_{\rm bol}$ for the primary component in Table 4, we calculated the observed pulsation constants

TABLE 6

RESULTS OF A MULTIPLE FREQUENCY ANALYSIS OF BBAND RESIDUALS

Frequency[a] (cycles day^{-1})	Amplitude[a] (mag)	Phase[a] (rad)	S/N$_1$[a]	S/N$_2$[a]
$f_1 = 32.69236$	0.0034	4.94	8.9	7.3
± 0.00006	± 0.0002	± 0.05	...	...
$f_2 = 36.65999$	0.0027	6.01	7.8	7.6
± 0.00006	± 0.0002	± 0.06	...	...
$f_3 = 20.71649$	0.0018	1.34	5.3	5.1
± 0.00009	± 0.0002	± 0.10	...	...
$f_4 = 30.66072$	0.0016	4.48	4.3	3.5
± 0.00011	± 0.0002	± 0.11	...	...
Standard deviation	...	0.0051 mag	...	...

[a] Frequencies (f_j), amplitudes (A_j), and phases (ϕ_j) are values of the equation $m = m_0 + \Sigma_j A_j \cos\{2\pi f_j (t - t_0) + \phi_j\}$, $t_0 =$ HJD 2,453,000.0.

[b] The S/N were calculated from two different noise levels: S/N$_1$ averaging noises in whole frequency span between 0 and 50 cycles day^{-1} and S/N$_2$ using 5 cycles day^{-1} boxes around each frequency.

from the following equation: $\log Q_j = -\log f_j + 0.5 \log g + 0.1\ M_{\rm bol} + \log T_{\rm eff} - 6.456$ (Breger 2000); $Q_1 = 0.0139$, $Q_2 = 0.0124$, $Q_3 = 0.0219$, and $Q_4 = 0.0148$. The errors of these values were estimated to be about 6%, around ± 0.0010 days. We compared these values with the theoretical one by Fitch (1981), adopting a 2.0M43 model with similar physical parameters to IV Cas, but in a more evolved stage. The corresponding radial orders are $n = 2$ (f_3) and $n = 4$–5 (f_1, f_2, and f_4).

The spherical harmonic degree ℓ can be determined by comparing the phase differences and amplitude ratios between multiple passbands (Rodríguez et al. 1996, 2004b, 2010). We calculated these indices for the four frequencies of IV Cas. They were in the range of $A_B/A_V = (1.3 \sim 0.9) \pm 0.2$ and $\phi_B - \phi_V = (-0.3 \sim 0.1) \pm 0.2$ rad. Comparing with the theoretical values by Rodríguez et al. (2010, their Fig. 10), the indices placed roughly $\ell = 0 \sim 2$ modes. Unfortunately, we failed to get a reliable ℓ value for each frequency of IV Cas, due to the large errors on these indices.

The frequency difference of $f_2 - f_1 = 3.96763$ cycles day^{-1} is nearly 2 times the other frequency difference $f_1 - f_4 = 2.03164$ cycles day^{-1}. The differences are very close to 4.0 and 2.0 cycles day^{-1}, but we believe that it does not result from the aliasing frequencies due to data sampling or from the false splitting frequencies due to the dilution effect (see § 4.1). The same frequency pattern has been found at other pulsating stars such as 29 Cyg (Mkrtichian et al. 2007) and Y Cam (Rodríguez et al. 2010). Therefore, we can interpret the differences in the same way, i.e., the frequency spacing of 4.0 cycles day^{-1} (=46 μHz) as the spacing between consecutive overtones of the same degree ℓ (so-called large frequency separation) and half-frequency spacing as the spacing of consecutive even or odd ℓ values. The large separation scales roughly as $(M/R^3)^{1/2}$ and is expected to be 61 ± 2 μHz for IV Cas, applying 135 μHz for the Sun. The discrepancy between the observed and

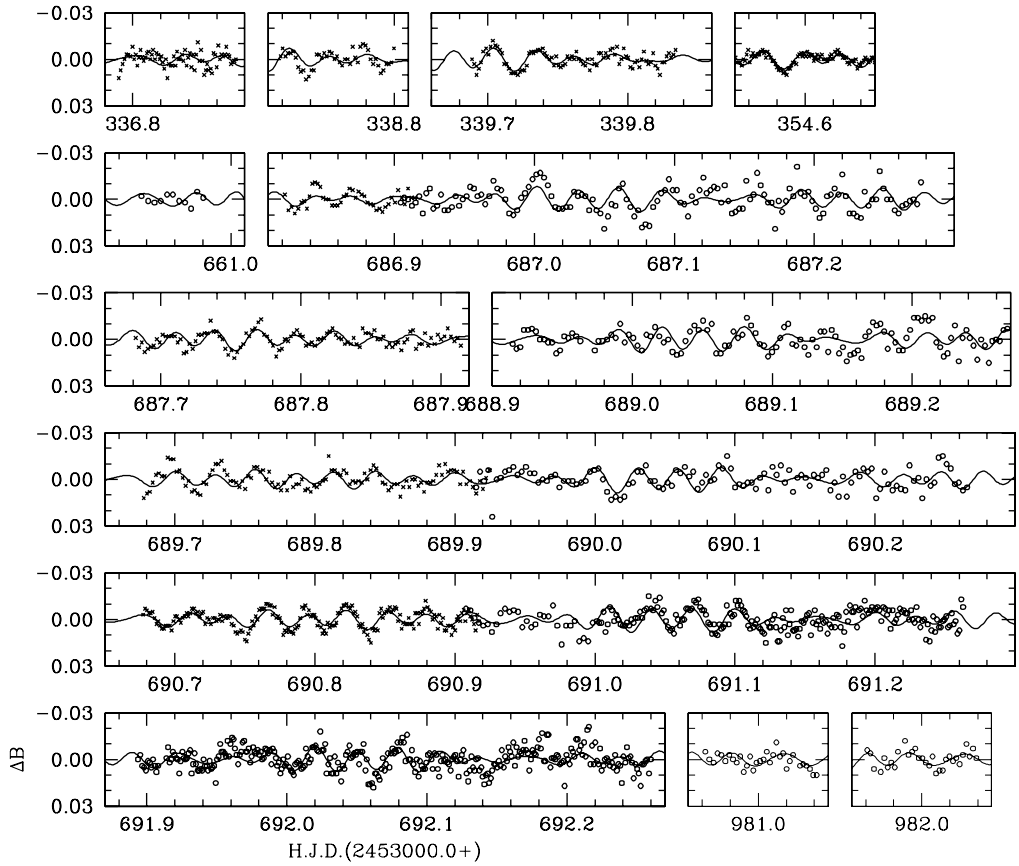

FIG. 4.—Observed and synthetic light variations of B-band residuals in the out-of-primary eclipsing phases. Open circles denote observed data from SOAO and crosses are data from LOAO. The synthetic curves were calculated from a multiple-frequency analysis.

expected values is quite large, indicating that the differences do not originate from the large frequency separation.

In the case of nonradial oscillations, nearly equal frequency spacing can be explained in terms of a rotational splitting with the same n and ℓ numbers but differing azimuthal order m. The asymptotic first-order approximation, applied to a star rotated as a solid body, gives the splitting $\delta\nu_{\rm nlm}$ as being simply proportional to the stellar rotation rate, $\delta\nu_{\rm nlm} = -mf_{\rm rot}$. Hereafter, we set the prograde modes as $m < 0$. The primary component of IV Cas may rotate synchronously with the revolution (see the next section) and then its rotation rate becomes $f_{\rm rot} \sim 1.0$ cycles day^{-1}. Therefore, the three frequencies f_1, f_2, and f_4 can be identified as the rotational splitting with the same n and ℓ values but differing $m = 0$, -4, and $+2$, respectively. However, this identification is rather unreasonable, because the disk-integrated photometric amplitudes decrease strongly for modes with ℓ (also m) greater than 2. On the other hand, for equator-on-visible stars, like the pulsating components in eclipsing binaries, the disk-integrated amplitudes of $(\ell + |m|)$ being odd modes tend to be close to zero, meaning that only the radial and $(\ell, m) = (l, \pm1)$, (2, $\pm$2), (2, 0) nonradial modes can survive in the signal integrated over the stellar disk (Mkrtichian et al. 2004). Accordingly, we identified f_1 and f_4 as the rotational splitting frequencies with $(\ell, m) = (1, -1)$ and (1, +1) or $(\ell, m) = (2, -2)$ and (2, 0), respectively, and f_2 has a higher radial order than f_1 and f_4. It is also possible that f_1 and f_2 are the rotational splitting frequencies with $(\ell, m) = (2, +2)$ and (2, $-$2), respectively, and f_4 has a lower radial order than f_1 and f_2.

As a result, we tentatively identified the most plausible pulsation modes as $(n, \ell, m) = (4, 2, -2)$ for f_1, (5, 0, 0) for f_2, (2,1,$-$1) for f_3, and (4, 2, 0) for f_4, accepting that f_1 and f_4 are rotational splitting frequencies. For these modes, the difference between theoretical and observed pulsation constants was estimated to be $\Delta Q = 0.0002 \pm 0.0002$, showing good consistency; we recalculated the observed pulsation constants to correct for the rotational splitting effect as follows, $f_{j,\rm cor} = f_{j,\rm obs} + mf_{\rm rot}$. If we assume another possibility that f_1 and f_2 are rotational splitting frequencies, the pulsation modes become $(n, \ell, m) = (5, 2, +2)$ for f_1, (5, 2, $-$2) for f_2, (2, 1, $-$1) for f_3, and (4, 2, 0) for f_4, and the difference is $\Delta Q = 0.0003 \pm 0.0001$. The other case mentioned in the former paragraph, $(\ell, m) = (1, -1)$ for f_1 and (1, +1) for f_4, showed the large value of $\Delta Q = -0.0013 \pm 0.0002$.

5. DISCUSSION

We studied the evolutionary status of IV Cas. The absolute parameters of both components were compared with the mass-radius, mass-luminosity, and Hertzsprung-Russell (HR) diagrams (cf. İbanoğlu et al. 2006). In these diagrams, the primary star lies between the zero-age main sequence and the terminal-age main sequence (TAMS), while the secondary is slightly beyond TAMS: a location where the secondary components of some other Algol-type binaries are found. The secondary component is oversize by a factor of about 2 and more than four times too luminous, compared with main-sequence stars of the same mass. Our results reveal that IV Cas is an Algol-type semidetached binary system, consisting of a detached main-sequence primary of spectral type A3 and an evolved secondary of early-K spectral type, which fills its inner Roche lobe completely. Such a configuration supports the concept of mass transfer from the secondary to the primary component. However, the detached primary star is located far above the ω_d curve, the disk radii expected from the hydrodynamic computations of Lubow & Shu (1975), in a plot of fractional radius of a gainer versus mass ratio. This implies that the two components are too close to each other to form an accretion disk. Spectroscopic results without an emission feature also indicate that there is no noticeable accretion disk around the primary component (see § 3.1).

A strong tidal force in close binaries like IV Cas makes the rotation of each component synchronized with the revolution. Most secondary components that have filled their Roche lobe are synchronized. However, several primary components, even in evolved (i.e., semidetached or contact) binary configurations, appear to rotate significantly faster than expected in the case of synchronism (Giuricin et al. 1984). A possible explanation for the asynchronism is that primary components spin up due to the transfer of angular momentum from the mass-losing secondary during the rapid mass transfer phase and are at the beginning of a slow mass transfer phase, not yet in synchronism (Mkrtichian et al. 2002). Our study of IV Cas, $F_{\rm asyn} = v_{\rm obs}/v_{\rm syn} = v_{\rm rot} \sin i_{\rm orb}/(2\pi R/P_{\rm orb}) \sim 1.06$, shows that the rotation of the primary component is nearly synchronous with the revolution, considering the errors in the observed rotation velocity and estimated radius. Here, we assume that the rotation axis is perpendicular to the orbital plane. The synchronism of the primary gives a hint that IV Cas is in the middle or late stage of the slow mass transfer phase. This coincides well with a slow mass transfer rate deduced from the fact that the eclipsing minimum epochs collected for about 100 yr do not show a secular parabolic variation in the O-C diagram (see § 3.3).

Like many of the oEA stars shown in Figure 1 of Soydugan et al. (2006a), the primary component of IV Cas is located close to the blue edge of the δ Scuti instability strip in the HR diagram. It has the typical pulsation properties of the oEA stars in that region. Soydugan et al. (2006a) discovered two empirical relations between pulsation periods and orbital periods and between pulsation periods and gravitational forces (see their Figs. 2 and 3). For IV Cas, the gravitational force (pull) exerted per gram of matter on the surface of the primary component by the secondary was calculated to be $\log F_{\rm grav} = 3.19$ in cgs units. The dominant pulsation period of about 0.0306 day, the orbital period of about 0.9985 day, and the gravitational force well match these empirical relations.

The ratios between orbital and pulsation periods of IV Cas depart clearly from integer values, in contrast with what is expected if some resonance is present. This indicates that the hypothesis of pulsation-to-orbital synchronization (POS) by tidal resonance does not apply to the eclipsing binary IV Cas. Observational evidences of the POS have been reported restrictively in few eclipsing binaries: for example, V6 in the open cluster NGC 2126 (Gáspár et al. 2003) with the ratio of 9.07 and AI Hya with that of 60.06 (Jorgensen & Gronbech 1978).

We greatly appreciate an anonymous referee for the valuable comments. This research made use of the SIMBAD database, operated at CDS, Strasbourg, France.

REFERENCES

Brát, L., Šmelcer, L., & Kuèáková, H., et al. 2008, Open Eur. J. Var. Stars, 94, 1
Breger, M. 2000, in ASP Conf. Ser. 210, Delta Scuti and Related Stars, ed. M. Breger, & M. H. Montgomery, 3
Breger, M., Stich, J., & Garrido, R., et al. 1993, A&A, 271, 482
Brown, T. M., & Gilliland, R. L. 1994, ARA&A, 32, 37
Cunha, M. S., Aerts, C., & Christensen-Dalsgaard, J., et al. 2007, A&A Rev., 14, 217
Dimitrov, D., Kraicheva, Z., & Popov, V. 2009, IBVS, 5883, 1
Erkan, N., Erdem, A., Akin, T., Aliçavus, F., & Soydugan, F. 2010, IBVS, 5924, 1
Fitch, W. S. 1981, ApJ, 249, 218
Gáspár, A., Kiss, L. L., & Bedding, T. R., et al. 2003, A&A, 410, 879
Giuricin, G., Mardirossian, F., & Mezetti, M. 1984, A&A, 131, 152
Gray, R. O., & Corbally, C. J. 1994, AJ, 107, 742
Harmanec, P. 1988, Bull. Astron. Inst. Czechoslovakia , 39, 329
Hübscher, J., Steinbach, H.-M., & Walter, F. 2009, IBVS, 5874, 1
İbanoğlu, C., Soydugan, F., Soydugan, E., & Dervişoğlu, A. 2006, MNRAS, 373, 435
Jorgensen, H. E., & Gronbech, B. 1978, A&A, 66, 377
Kim, K. M., Mkrtichian, D. E., Lee, B.-C., Han, I., & Hatzes, A. P. 2006a, A&A, 454, 839
Kim, S.-L., & Lee, S.-W. 1996, A&A, 310, 831
Kim, S.-L., Lee, C.-U., Koo, J.-R., et al. 2005, IBVS, 5669, 1
Kim, S.-L., Lee, J. W., Kwon, S.-G., Youn, J.-H., Mkrtichian, D. E., & Kim, C. 2003, A&A, 405, 231
Kim, S.-L., Lee, C.-U., & Lee, J. W. 2006b, Mem. S.A. It., 77, 184
Kim, S.-L., Lee, J. W., Youn, J.-H., Kwon, S.-G., & Kim, C. 2002, A&A, 391, 213

Kurucz, R. L. 1993, Kurucz CD-ROM 13, ATLAS9 Stellar Atmosphere Programs and 2 km/s Grid (Cambridge: Smithsonian Astrophys. Obs.), http://kurucz.harvard.edu
Kwee, K. K., & van Woerden, H. 1956, Bull. Astron. Inst. Netherlands, 12, 327
Lampens, P. 2006, in ASP Conf. Ser. 349, Astrophysics of Variable Stars, ed. C. Sterken, & C. Aerts, 153
Lampens, P., Strigachev, A., & Kim, S.-L., et al. 2010, A&A, submitted
Le Borgne, J.-F., Bruzual, G., & Pello, R., et al. 2003, A&A, 402, 433
Lee, J. W., Kim, C.-H., & Koch, R. H. 2007, MNRAS, 379, 1665
Lee, J. W., Kim, S.-L., Lee, C.-U., Kim, H.-I., Park, J.-H., Park, S.-R., & Koch, R. H. 2009, PASP, 121, 104
Lee, C.-U., Kim, S.-L., & Lee, J. W., et al. 2008, MNRAS, 389, 1630
Lehmann, H., & Mkrtichian, D. E. 2008, A&A, 480, 247
Lenz, P., & Breger, M. 2005, CoAst, 146, 53
Liakos, A., & Niarchos, P. 2009, CoAst, 160, 2
Lubow, S. H., & Shu, F. H. 1975, ApJ, 198, 383
Mkrtichian, D. E., Kusakin, A. V., Gamarova, A. Y., & Nazarenko, V. 2002, in ASP Conf. Ser. 259, Radial and Nonradial Pulsations as Probes of Stellar Physics, ed. C. Aerts, T. R. Bedding, & J. Christensen-Dalsgaard (San Francisco: ASP), 96
Mkrtichian, D. E., Kusakin, A. V., & Lopez de Coca, P., et al. 2007, AJ, 134, 1713
Mkrtichian, D. E., Kusakin, A. V., & Rodriguez, E., et al. 2004, A&A, 419, 1015
Pigulski, A. 2006, in ASP Conf. Ser. 349, Astrophysics of Variable Stars, ed. C. Sterken, & C. Aerts (San Francisco: ASP), 137
Rodríguez, E., García, J. M., & Costa, V., et al. 2010, MNRAS, submitted
Rodríguez, E., García, J. M., & Gamarova, A. Y., et al. 2004b, MNRAS, 353, 310
Rodríguez, E., García, J. M., & Mkrtichian, D. E., et al. 2004a, MNRAS, 347, 1317
Rodríguez, E., López-González, M. J., & López de Coca, P. 2000, A&AS, 144, 469
Rodríguez, E., Rolland, A., López de Coca, P., & Martín, S. 1996, A&A, 307, 539
Royer, F., Zorec, J., & Gómez, A. E. 2007, A&A, 463, 671
Samus, N. N.et al. 2009, General Catalogue of Variable Stars (Moscow: Sternberg Astron. Inst.), http://www.sai.msu.su/groups/cluster/gcvs/gcvs/
Soydugan, E., İbanoglu, C., Soydugan, F., Akan, M. C., & Demircan, O. 2006a, MNRAS, 366, 1289
Soydugan, E., Soydugan, F., Demircan, O., & İbanoglu, C. 2006b, MNRAS, 370, 2013
Soydugan, E., Soydugan, F., Senyüz, T., Püsküllü, C., Tüysüz, M., Bakis, V., Bilir, S., & Demircan, O. 2009, IBVS, 5902, 1
Svechnikov, M. A., & Kuznetsova, Eh. F. 1990, Sverdlovsk, 1, 2
Van Hamme, W. 1993, AJ, 106, 2096
Wilson, R. E., & Biermann, P. 1976, A&A, 48, 349
Wilson, R. E., & Devinney, E. J. 1971, ApJ, 166, 605
Wolf, M., Zejda, M., Kiyota, S., Maehara, H., Nagai, K., & Nakajima, K. 2006, IBVS, 5735, 1